Fermi National Accelerator Laboratory

FERMILAB-Conf-88/194
[SSC-197]

Thermal Performance Measurements of a Graphite Tube Compact Cryogenic Support for the Superconducting Super Collider*

J. D. Gonczy, W. N. Boroski, E. T. Larson, T. H. Nicol,
R. C. Niemann, J. G. Otavka, and M. K. Ruschman
Fermi National Accelerator Laboratory
P.O. Box 500, Batavia, Illinois 60510

December 1988

*Presented by J. D. Gonczy at ICEC 12, Southampton, England, July 12-15, 1988.

Operated by Universities Research Association Inc. under contract with the United States Department of Energy

THERMAL PERFORMANCE MEASUREMENTS OF A GRAPHITE TUBE COMPACT CRYOGENIC SUPPORT FOR THE SUPERCONDUCTING SUPER COLLIDER

J.D. Gonczy, W.N. Boroski, E.T. Larson, T.H. Nicol, R.C. Niemann, J.G. Otavka, and M.K. Ruschman

Fermi National Accelerator Laboratory, Batavia, IL, USA

The magnet cryostat development program for the Superconducting Super Collider (SSC) High Energy Physics Proton-Proton Collider has produced an innovative design for the structural support of the cold mass and thermal radiation shields. This work updates the continuing development of the support known as the Compact Cryogenic Support (CCS). As the structural and thermal requirements of the SSC became better defined, a CCS was developed that employs an innermost tube comprised of a graphite composite material. Presented is the thermal performance to 4.5K of the graphite CCS model.

INTRODUCTION

Magnet system requirements for the SSC specify that the cryostat support system withstand potentially high bending loads which may occur during shipping and handling, or as a result of magnet quench during operation[1] The requirements also limit the support system conductive heat leak at 120mW to 4.5K, 820mW to 20K, and 7.2W to 80K. Optimization of the support system for structural and thermal performance has resulted in a CCS that uses composite tubes having greater wall thickness than earlier reported CCS models.[2] In addition, carbon-graphite reinforced plastic (CgRP) has replaced glass reinforced plastic (GRP) as the material comprising the innermost tube. The CgRP material has a higher modulus of elasticity than the GRP and lower thermal conductivity below 40K.[3] It therefore contributes a gain in stiffness for the CCS assembly and promises lower heat conduction to 20K and 4.5K. GRP remains the material of choice for the outer tube.

Reported herein is the thermal performance of a graphite CCS model that meets the structural requirements of the SSC. Described are two separate experimental measurements using different test arrangements and made on the CCS in a Heat Leak Test Facility (HLTF). In the first arrangement, the thermal performance of the graphite CCS was measured with the CCS cold end connected directly to 4.5K. In the second, the test was reconfigured to include the addition of a cold mass slide-connection attached to the CCS.[4] The geometry of the graphite CCS model, its instrumentation and experimental test arrangements in the HLTF are described. Reported are heat leak and temperature profile measurements made with the primary heat intercept temperature controlled at different steady-state temperature levels between 10K and 40K. Heat leak values to 4.5K were measured by means of a heatmeter.[5] Heat leak values to the primary and secondary heat intercepts were derived using the measured temperature profiles and component material properties. Also, presented are thermal performance measurements along copper cables used to sink the CCS heat intercepts to their respective primary and secondary thermal radiation shields.

OVERVIEW - CCS INSTALLATION IN THE SSC DIPOLE MAGNET CRYOSTAT

The compact cryogenic support is the main structural support member for the cold mass, and the primary (20K) and secondary (80K) thermal radiation shields (Figure 1 details the SSC magnet cross-section). Five support locations are used along the cold mass length. At the cold mass midspan, the center CCS is rigidly attached to the cold mass and thermal shields thereby anchoring the cryostat. Away from the midspan, the CCS attachments to the cold mass and shields are by means of sliding connections that preclude axial loading of the supports due to thermal contraction of the cold mass and

shields during cool down and warm-up. Flexible copper cables having crimped-on aluminum ends are used on each CCS to heat sink the shield support station to its respective shield. Conductive heat load along the CCS is thereby intercepted and directed to the shields. Two cables thermally anchor each CCS to the primary shield; six cables anchor each CCS to the 80K shield. The cable connections are terminated at the CCS and shields by aluminum welding.

5x7 CgRP/GRP CCS MODEL DESCRIPTION AND TEST INSTRUMENTATION

The CCS design description (illustrated in the cross-sectioned view in Figure 2) has been documented in detail.[7] Briefly, it consists of two concentric composite tubes; one operating between 300K and 80K, the other between 80K and 4.5K. A metallic tubular element bridges the 80K connection between inner and outer composite tubes and accomplishes the reentrance of the conduction heat path within the outer tube, thereby adding length to the path without compromising vertical height. Multilayer insulation internal to the CCS limits radiant heat transfer between components. The metallic ends and shield support stations are joined to the composite tubes by clamping pressure generated from dimensional interferences between components at the joint locations. Thermal shrink fitting techniques are used to assemble the cryogenic support resulting in joints that are nonintrusive to the composite tubes. No other mechanical or chemical bonds are made to the composite tubes.

The composite tubes in these tests were manufactured by Keystone Engineering Co., Houston, Texas, USA. The innermost tube was made using bi-directional graphite T300-3K, 12.5 x 12.5 plain weave fabric. The outermost tube used a satin weave E-glass, 57 x 54 construction. Both resin systems used an epoxy with an amine cure.

TEMPERATURE PROFILE AND HEAT LEAK MEASUREMENTS

The CCS temperature profile and heat leak measurements were conducted in the Heat Leak Test Facility. The HLTF provides the thermal connections to 4.5K, 20K, 80K, and 300K that replicate the CCS installation in an SSC cryostat.[8]

Shown in Table 1 are the locations of 23 temperature sensors installed along the conductive heat path of the CCS. The sensors are used to generate dynamic temperature profiles, (Reference Figures 5a-h) which are measured along the composite tubes and across the shrink-fit joints, and which show the thermal tracking relationship of components within the CCS. Carbon resistors measure temperatures from 4.5K to approximately 50K; platinum resistors are used above 50K. A computerized data acquisition system records experimental data.

Figure 3 illustrates the HLTF test geometry with the 5x7 CgRP/GRP CCS connected directly to the heatmeter at 4.5K. The results of thermal performance measurements with the primary heat intercept at different steady-state temperature levels are listed in Table 1. Heat leaks are by measurement with the heatmeter and by calculation using the measured temperatures with material properties of thermal conductivity.

The test was reconfigured as in Figure 4 using the same CCS with the addition of a cold mass slide-connection attachment having a copper simulated cold mass. The temperature profiles and heat leak values for these measurements are listed in Table 2.

Figures 5a-5h describe dynamic parameters measured to steady-state conditions for the primary intercept temperature of 22.5K found in Table 2. Explanation of the different graphs is by title. The numbers within parentheses on plots 5b, 5c, and 5e correspond to numbered sensors along the CCS as illustrated in Table 2. Figure 5h shows the response of the heatmeter to 30mW of electrical power from a calibration heater on the simulated cold mass.

Figure 6 plots heat leak to 4.5K versus primary shield temperatures for measurements in the two test arrangements.

DISCUSSION

The heat leak measured by the heatmeter was higher by 5-8mW with the slide attachment. (See Figure 6). The higher heat load is attributed to residual gas conduction to the much larger surface areas as afforded by the slide-connection and the cold mass assemblies. Solid conduction through instrumentation wires to temperature sensors on the slide-connection and simulated cold mass, and to the calibration heater also contributed to the higher heat leak values.

The measured operating temperature of the metal tube component in the CCS is significantly higher than predicted by design. This heat gain is attributed to thermal radiation, and poor heat removal due to the low thermal conductance path across the wall of the outermost composite tube to the 80K heat sink, and results in a higher heat load to 20K.

CONCLUSIONS

- A CCS that meets the structural requirements of the SSC has been thermally evaluated and found to nearly meet the requirements of the heat leak budget.
- The cold mass slide-connection offers negligible thermal impedance and therefore negligible heat leak reduction for the CCS assembly.
- The copper cables that thermally anchor the CCS heat intercepts to their respective shields performed well, measuring a 1K temperature drop across the cable to 20K, and about 2.5K drop to 80K.
- Heat leak to 20K can be reduced by relocating the 80K heat sink cables from their connection at the CCS secondary shield support station to a direct connection on the metal tube between composite tubes; increased wall thickness on the metal tube will also help.

ACKNOWLEDGEMENTS

The authors express their appreciation to Messr. C. Schoo for his help and dedication in testing the CCS model, and to Messr. C. Grimm for the illustrations in this work.

REFERENCES

1 SSC Central Design Group, 'Superconducting super collider magnet system requirements' SSC-MAG-D-101 (July 23, 1987).

2 Gonczy, J.D., et al., 'Cryogenic support thermal performance measurements'. Adv. in Cryo. Eng., vol. 33 (1988), pp. 243-250.

3 Takeno, et al., 'Thermal and mechanical properties of advanced composite materials at low temperature'. Adv. in Cryo. Eng., vol. 32 (1986), pp. 217-224.

4 Larson, E.T., et al., 'Improved design for a SSC coil assembly suspension connection'. Adv. in Cryo. Eng., vol. 33 (1986), pp. 235-241.

5 Kuchnir, M., et al., 'Measuring heat leak with a heatmeter'. Adv. in Cryo. Eng., Vol. 31 (1986), pp. 1285-1290.

6 Niemann, R.C., et al., 'Superconducting super collider magnet cryostat'. Cryogenic Properties, Processes and Applications, No. 251, vol. 82 (1986), pp. 166-171.

7 Nicol, et al., 'SSC magnet cryostat suspension system design'. Adv. in Cryo, Eng., vol. 33 (1988), pp. 227-234.

8 Gonczy, J.D., 'Heat leak measurement facility'. Adv. in Cryo. Eng., vol. 33 (1986), pp. 1291-1298.

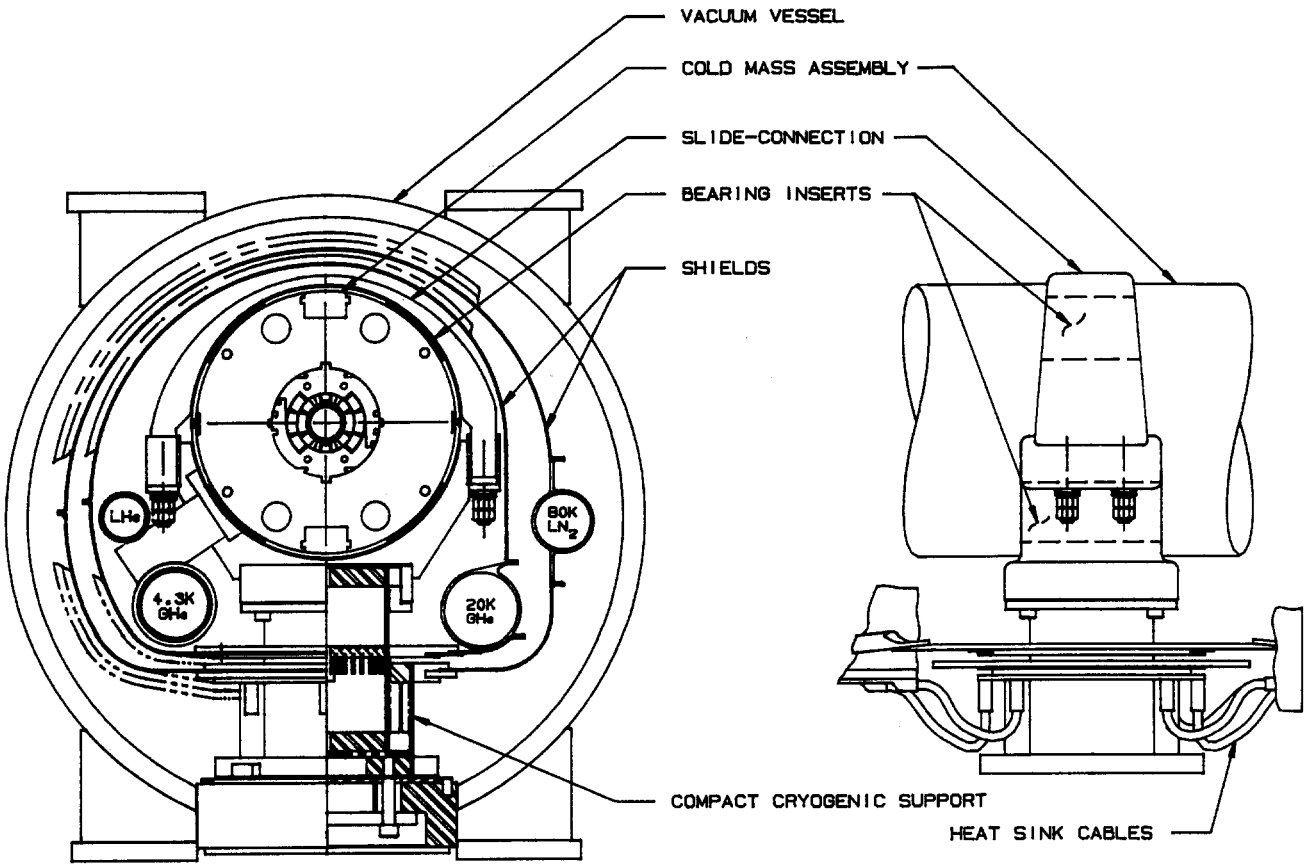

Fig. 1. SSC Magnet cross-section

Fig. 2. CCS cross-section.

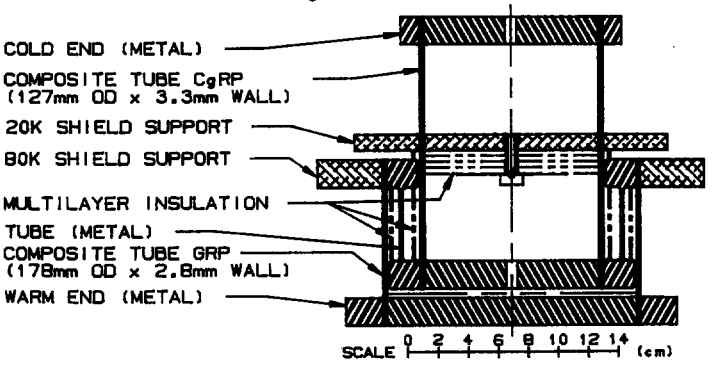

Fig. 3. HLTF - CCS connection directly to 4.5K.

Fig. 4. HLTF - CCS with slide cradle attachment.

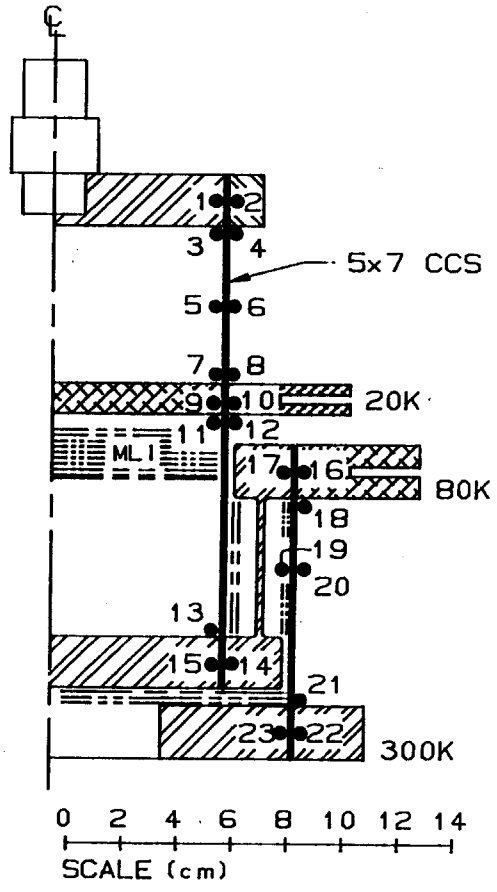

5x7 CgRP/GRP CCS TEMPERATURE PROFILE MEASUREMENTS (K)										
SENSOR NUMBER	SENSOR TYPE	DESIGN TEMP. (K)	PRIMARY INTERCEPT TEMPERATURE (K)							
			11.5	14.2	17.9	22.3	22.8	25.4	32.6	34.7	40.7
1	CARBON RES.	4.5	5.5	5.9	6.3	7.0	6.9	7.4	8.6	9.0	10.3
2	CARBON RES.	4.5	5.7	6.1	OPEN	7.3	7.3	7.8	9.2	9.6	11.2
3	CARBON RES.	4.9	6.6	7.4	8.4	9.9	9.9	11.0	13.8	14.7	17.7
4	CARBON RES.	4.9	6.4	7.1	OPEN	9.3	9.3	10.1	12.7	13.5	16.0
5	CARBON RES.	13.6	9.4	11.2	13.6	16.7	16.9	18.7	24.2	25.8	30.7
6	CARBON RES.	13.6	OPEN	OPEN	OPEN	OPEN	OPEN	OPEN	OPEN	OPEN	OPEN
7	CARBON RES.	20.0	11.9	14.3	17.7	21.7	22.2	24.6	31.4	33.4	39.1
8	CARBON RES.	20.0	12.2	14.7	OPEN	22.1	22.5	24.9	32.3	34.6	41.4
9	CARBON RES.	20.0	15.8	17.8	20.8	24.8	25.2	27.3	34.0	35.9	41.4
10	CARBON RES.	20.0	11.5	14.2	17.9	22.3	22.8	25.4	32.6	34.7	40.7
11	CARBON RES.	20.0	31.7	32.7	34.1	36.7	36.7	37.9	42.0	43.0	46.6
12	CARBON RES.	20.0	OPEN	OPEN	OPEN	OPEN	OPEN	OPEN	OPEN	OPEN	OPEN
13	Pt RTD	79.0	81.4	81.4	81.5	81.6	81.6	81.6	82.2	82.1	82.6
14	Pt RTD	79.1	89.7	89.7	89.8	89.7	89.7	89.7	90.0	89.8	90.1
15	Pt RTD	79.1	85.3	85.3	85.4	85.4	85.4	85.4	85.7	85.5	85.7
16	Pt RTD	80.0	82.8	83.0	83.0	82.9	82.9	82.9	83.1	82.9	83.0
17	Pt RTD	80.0	85.5	85.6	85.6	85.5	85.5	85.5	85.8	85.7	85.7
18	Pt RTD	80.8	110.5	110.5	110.5	110.6	110.5	110.5	110.7	110.6	110.7
19	Pt RTD	200.0	203.5	203.4	203.2	203.6	203.4	203.5	203.7	203.6	203.5
20	Pt RTD	200.0	203.0	203.0	203.8	203.2	203.0	203.2	203.3	203.2	203.1
21	Pt RTD	299.7	271.9	271.8	271.4	272.1	271.7	272.0	272.2	272.1	272.0
22	Pt RTD	300.0	286.1	286.0	285.5	286.3	285.9	286.2	286.4	286.3	286.3
23	Pt RTD	300.0	286.9	286.8	286.3	287.1	286.7	287.0	287.2	287.1	287.0
HEAT LEAK MEASUREMENTS (mW) BY HEATMETER & MATERIAL PROPERTIES										
Q_{Hm}			8	11	16	25	23	31	50	54	80
Q_2			8	11	–	25	26	32	55	63	90
Q_{10}			447	440	–	414	412	401	362	344	297
Q_{16}			1653	1653	–	1670	1666	1675	1693	1702	1722

Table 1. 5 X 7 CgRP/GRP CCS thermal performance with CCS connected directly to 4.5K. illustrated are sensors along conduction heat path. Tabulated are measured temperatures and heat leak values at steady-state conditions.

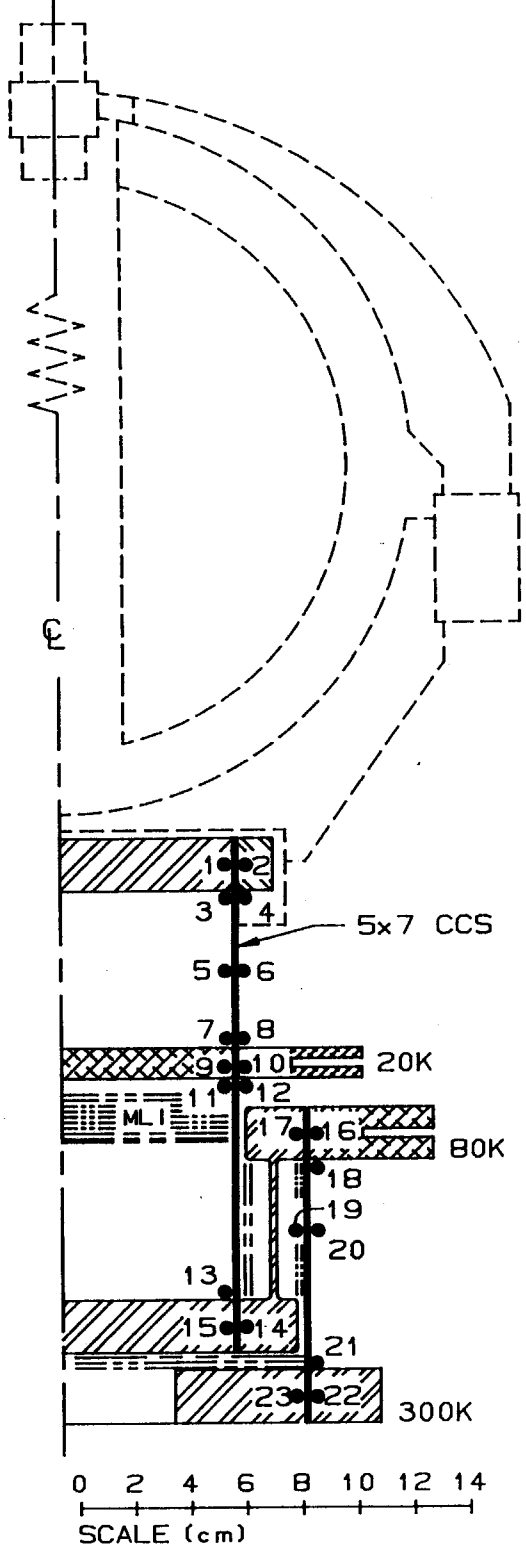

5x7 CgRP/GRP CCS WITH SLIDE – TEMPERATURE PROFILE MEASUREMENTS (K)									
SENSOR NUMBER	SENSOR TYPE	DESIGN TEMP. (K)	PRIMARY INTERCEPT TEMPERATURE (K)						
			11.4	13.4	22.5	23.2	27.1	31.7	32.6	37.9
1	CARBON RES.	4.5	6.2	6.5	8.0	9.4	8.9	9.9	10.1	11.5
2	CARBON RES.	4.5	6.3	6.6	8.3	9.7	9.2	10.3	10.5	12.0
3	CARBON RES.	4.9	6.9	7.5	10.2	11.5	11.9	13.6	13.9	16.2
4	CARBON RES.	4.9	6.9	7.3	9.8	11.2	11.3	13.0	13.3	15.3
5	CARBON RES.	13.6	9.5	10.7	16.8	17.7	19.9	23.5	24.2	28.2
6	CARBON RES.	13.6	9.3	10.4	16.4	17.3	19.5	22.8	23.4	27.6
7	CARBON RES.	20.0	11.9	13.5	21.9	22.6	26.2	30.5	31.3	36.5
8	CARBON RES.	20.0	12.2	13.9	22.2	22.9	26.7	31.2	32.2	38.2
9	CARBON RES.	20.0	15.9	17.4	25.0	25.6	28.9	33.2	34.0	38.9
10	CARBON RES.	20.0	11.4	13.4	22.5	23.2	27.1	31.7	32.6	37.9
11	CARBON RES.	20.0	30.9	31.7	35.8	36.2	38.2	40.8	41.4	44.6
12	CARBON RES.	20.0	OPEN	OPEN	OPEN	OPEN	OPEN	OPEN	OPEN	OPEN
13	Pt RTD	79.0	83.1	83.1	83.0	83.4	83.5	83.5	83.8	84.2
14	Pt RTD	79.1	91.2	91.1	90.9	91.2	91.2	91.1	91.4	91.5
15	Pt RTD	79.1	87.2	87.2	86.9	87.3	87.2	87.2	87.4	87.6
16	Pt RTD	80.0	84.9	84.8	84.5	84.9	84.8	84.6	84.9	85.0
17	Pt RTD	80.0	86.8	86.7	86.4	86.7	86.7	86.5	86.8	86.9
18	Pt RTD	80.8	110.3	110.2	109.9	110.2	110.2	110.1	110.3	110.4
19	Pt RTD	200.0	204.0	203.8	203.6	203.8	203.9	204.1	204.0	204.2
20	Pt RTD	200.0	201.3	201.0	200.9	201.1	201.2	201.4	201.3	201.5
21	Pt RTD	299.7	267.7	267.3	267.2	267.5	267.6	268.0	267.7	267.9
22	Pt RTD	300.0	281.9	281.6	281.5	281.8	282.0	282.3	282.0	282.3
23	Pt RTD	300.0	282.6	282.3	282.2	282.5	282.6	283.0	282.7	283.0

HEAT LEAK MEASUREMENTS (mW) BY HEATMETER & MATERIAL PROPERTIES								
Q_{HM}	13	15	30	CALIB.	41	56	58	80
Q_2	7	9	25	24	35	50	53	75
Q_{10}	466	460	429	431	412	383	381	341
Q_{16}	1566	1566	1583	1582	1594	1613	1607	1628

Table 2. 5 X 7 CgRP/GRP CCS with slide cradle attachment - illustrated are sensor locations. Tabulated are measured temperature profiles with associated heat leak values at steady-state conditions.

(a)

(b)

(c)

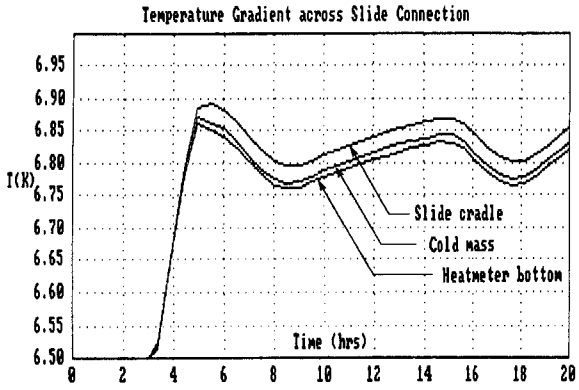

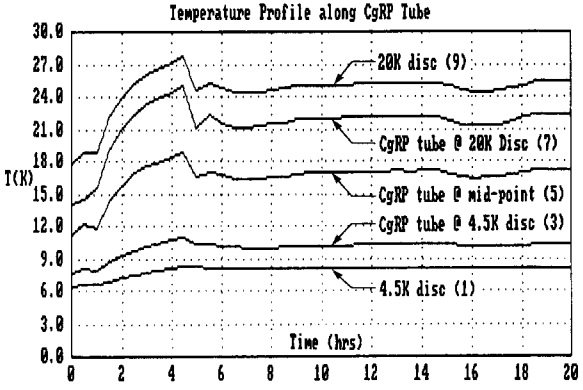

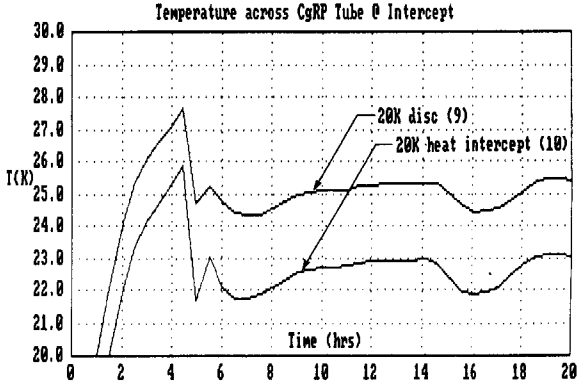

(d)

(e)

(f)

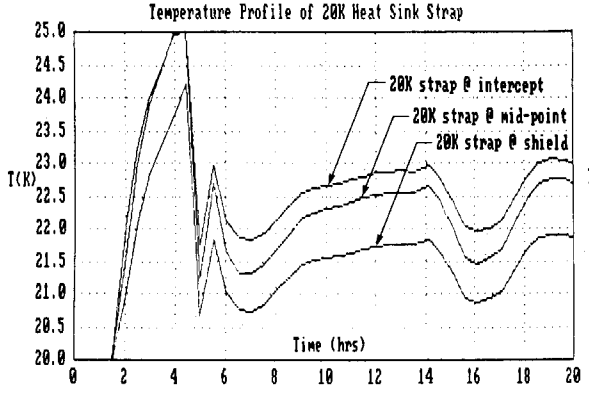

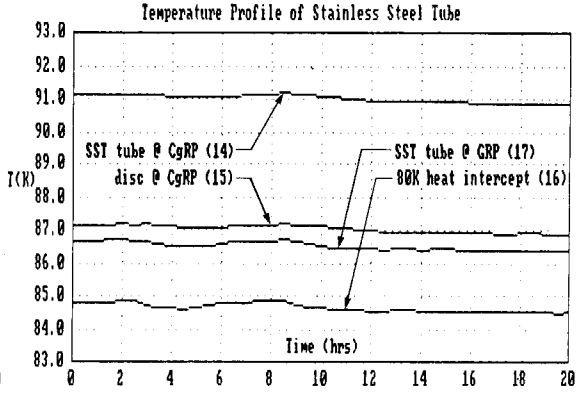

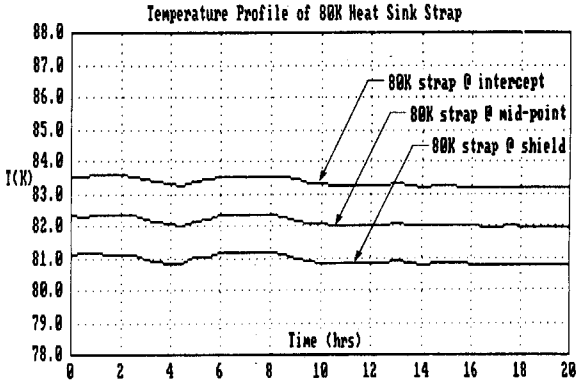

(g)

(h)

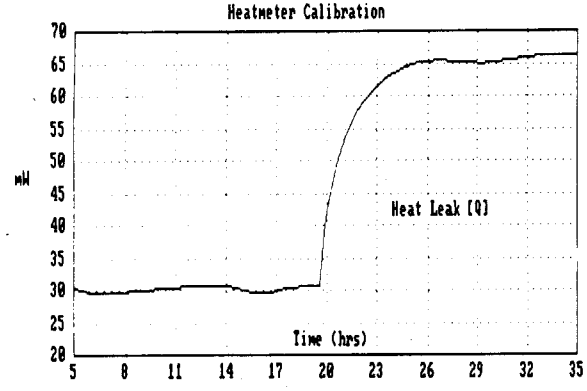

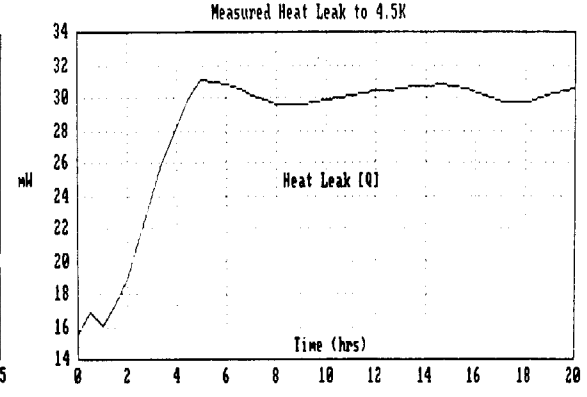

Fig. 5 (a-h). Dynamic parameters measured to steady-state conditions for the primary shield at 22.5K.

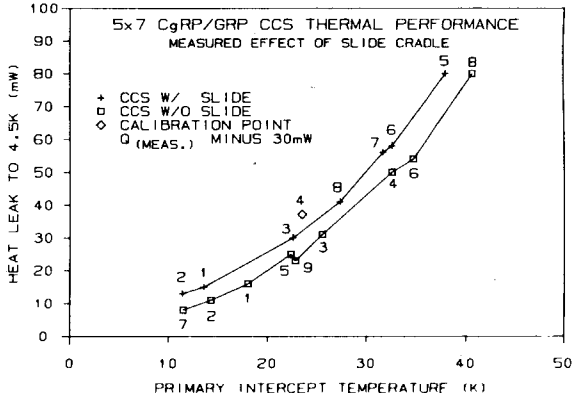

Fig. 6. Heat leak to 4.5K vs primary shield temperature.